HHS Public Access

Author manuscript

Cancer Res. Author manuscript; available in PMC 2020 January 07.

Published in final edited form as:

Cancer Res. 2018 April 01; 78(7): 1713–1725. doi:10.1158/0008-5472.CAN-17-1423.

Targeting the SphK1/S1P/S1PR1 Axis That Links Obesity, Chronic Inflammation, and Breast Cancer Metastasis

Masayuki Nagahashi[#1,2,3], **Akimitsu Yamada**[#2,3,4], **Eriko Katsuta**[2,5,3], **Tomoyoshi Aoyagi**[2,3], **Wei-Ching Huang**[2,3], **Krista P. Terracina**[2,3], **Nitai C. Hait**[3,5,6], **Jeremy C. Allegood**[3], **Junko Tsuchida**[1], **Kizuki Yuza**[1], **Masato Nakajima**[1], **Manabu Abe**[7], **Kenji Sakimura**[7], **Sheldon Milstien**[3], **Toshifumi Wakai**[1], **Sarah Spiegel**[3], **Kazuaki Takabe**[1,2,3,5,8,9,10]

[1]Division of Digestive and General Surgery, Niigata University Graduate School of Medical and Dental Sciences, Niigata City, Niigata, Japan.

[2]Division of Surgical Oncology, Department of Surgery, Virginia Commonwealth University School of Medicine, Richmond, Virginia.

[3]Departments of Biochemistry and Molecular Biology, Virginia Commonwealth University School of Medicine, Richmond, Virginia.

[4]Breast and Thyroid Surgery, Yokohama City University Medical Center, Kanagawa, Japan.

[5]Division of Breast Surgery, Department of Surgical Oncology, Roswell Park Comprehensive Cancer Center, Buffalo, New York.

[6]Department of Molecular and Cellular Biology, Roswell Park Comprehensive Cancer Center, Buffalo, New York.

[7]Department of Cellular Neurobiology, Brain Research Institute, Niigata University, Niigata City, Niigata, Japan.

[8]Department of Surgery, University at Buffalo Jacobs School of Medicine and Biomedical Sciences, The State University of New York, Buffalo, New York.

[9]Department of Breast Surgery and Oncology, Tokyo Medical University, Tokyo, Japan.

[10]Department of Surgery, Yokohama City University, Yokohama, Japan.

Corresponding Authors: Masayuki Nagahashi, Division of Digestive and General Surgery, Niigata University Graduate School of Medical and Dental Sciences, 1-757 Asahimachi-dori, Chuo-ku, Niigata City 951-8510, Japan. Phone: 812-5227-2228; Fax: 812-5227-0779; mnagahashi@med.niigata-u.ac.jp; and Kazuaki Takabe, Breast Surgery, Department of Surgical Oncology, Roswell Park Comprehensive Cancer Center, Buffalo, NY 14263. Phone: 716-845-2918; Fax: 716-845-1668; kazuaki.takabe@roswellpark.org.

Authors' Contributions

Conception and design: M. Nagahashi, K. Takabe

Acquisition of data (provided animals, acquired and managed patients, provided facilities, etc.): M. Nagahashi, A. Yamada, E. Katsuta, T. Aoyagi, W.-C. Huang, K.P. Terracina, N.C. Hait, J.C. Allegood, J. Tsuchida, K. Yuza M. Nakajima, M. Abe

Analysis and interpretation of data (e.g., statistical analysis, biostatistics, computational analysis): M. Nagahashi, T. Aoyagi, W.-C. Huang, J.C. Allegood, S. Spiegel, K. Takabe Writing, review, and/or revision of the manuscript: M. Nagahashi, K.P. Terracina, S. Milstien, S. Spiegel, K. Takabe

Administrative, technical, or material support (i.e., reporting or organizing data, constructing databases): M. Nagahashi, T. Aoyagi, W.-C. Huang, T. Wakai, K. Takabe

Study supervision: M. Nagahashi, K. Sakimura, T. Wakai, S. Spiegel, K. Takabe

Disclosure of Potential Conflicts of Interest

No potential conflicts of interest were disclosed.

Note: Supplementary data for this article are available at Cancer Research Online (http://cancerres.aacrjournals.org/).

[#] These authors contributed equally to this work.

Abstract

Although obesity with associated inflammation is now recognized as a risk factor for breast cancer and distant metastases, the functional basis for these connections remain poorly understood. Here, we show that in breast cancer patients and in animal breast cancer models, obesity is a sufficient cause for increased expression of the bioactive sphingolipid mediator sphingosine-1-phosphate (S1P), which mediates cancer pathogenesis. A high-fat diet was sufficient to upregulate expression of sphingosine kinase 1 (SphK1), the enzyme that produces S1P, along with its receptor S1PR1 in syngeneic and spontaneous breast tumors. Targeting the SphK1/S1P/S1PR1 axis with FTY720/fingolimod attenuated key proinflammatory cytokines, macrophage infiltration, and tumor progression induced by obesity. S1P produced in the lung premetastatic niche by tumor-induced SphK1 increased macrophage recruitment into the lung and induced IL6 and signaling pathways important for lung metastatic colonization. Conversely, FTY720 suppressed IL6, macrophage infiltration, and S1P-mediated signaling pathways in the lung induced by a high-fat diet, and it dramatically reduced formation of metastatic foci. In tumor-bearing mice, FTY720 similarly reduced obesity-related inflammation, S1P signaling, and pulmonary metastasis, thereby prolonging survival. Taken together, our results establish a critical role for circulating S1P produced by tumors and the SphK1/S1P/S1PR1 axis in obesity-related inflammation, formation of lung metastatic niches, and breast cancer metastasis, with potential implications for prevention and treatment.

Significance: These findings offer a preclinical proof of concept that signaling by a sphingolipid may be an effective target to prevent obesity-related breast cancer metastasis.

Introduction

Obesity has drastically increased to become one of the leading health concerns in the United States (1), and is now recognized as a risk factor for breast cancer incidence, progression, recurrence, and prognosis (2, 3). Epidemiologic and clinical studies indicate that obesity increases breast cancer risk by approximately 40% in postmenopausal women and is associated with endocrine therapy resistance (2, 4). Obese breast cancer patients are more likely to be diagnosed with larger, higher-grade tumors, have an increased incidence of distant metastases, and elevated risks of recurrence and death (3, 5). However, the mechanisms by which obesity increases breast cancer incidence and worsens prognosis remain ill defined.

High body weight has also been associated with larger and more aggressive tumors in animal models of breast cancer (6–10). Obesity in both humans and rodents is characterized by increased production of insulin and growth factors, low-grade chronic inflammation, and secretion of proinflammatory cytokines that regulate breast cancer development and progression (11–13). Animal models that recapitulate human cancers, such as syngeneic or transgenic murine models with intact immune functions, have provided important clues to the critical roles of the cytokines TNFα and IL6, and have highlighted the key roles played by the master transcription factors NFκB and STAT3 in the link between chronic inflammation and Nagahashi et al. breast cancer (14–16). Infiltration of macrophages (12)

that produce these cytokines into the tumor microenvironment is now recognized as an important enabler of cancer progression, and tumor-associated macrophages (TAM) correlate with increased angiogenesis, metastasis, and decreased survival of breast cancer patients (17). Macrophages have also been shown to be recruited to premetastatic niches, specialized microenvironments in distant organs primed by factors secreted from cancer cells that promote metastatic progression (18–20), but the underlying mechanisms guiding their assembly are largely unknown.

There is growing evidence that sphingosine-1-phosphate (S1P), a pleiotropic bioactive sphingolipid metabolite enriched both in blood and lymphatic fluid is involved in inflammation, obesity, and breast cancer (21). S1P generated by activation of sphingosine kinase 1 (SphK1) is exported out of cells and signals through specific S1P receptors to regulate numerous cellular processes important for breast cancer, including cell growth, survival, invasion, immune cell trafficking, vascular integrity, angiogenesis, and cytokine and chemokine production (22–25). Previous clinical studies have shown that SphK1 is overexpressed in breast cancer and its expression is associated with poor patient outcomes (26, 27). Because it has been suggested that S1P levels are elevated in plasma of obese humans and rodents (28), in this work we explored the role of S1P in obesity promoted breast cancer in patients and in animal models. We uncovered that the SphK1/S1P/S1PR1 axis is a critical factor linking obesity, low-grade chronic inflammation, and breast cancer, identified S1P as an important new factor in metastatic niche formation and demonstrated that targeting the SphK1/S1P/S1PR1 axis is an effective treatment for metastatic breast cancer exacerbated by obesity.

Materials and Methods

Cell culture

A C57Bl/6 mouse mammary fat pad–derived adenocarcinoma cell line E0771 was obtained from CH3 BioSystems. A BALB/c mouse mammary fat pad–derived adenocarcinoma cell line 4T1-luc2 that has been engineered to express luciferase was obtained from PerkinElmer. E0771 cells were cultured in DMEM with 10% FBS. 4T1-luc2 cells were cultured in RPMI medium 1640 with 10% FBS. SphK1 was overexpressed by transfection with Lipofectamine Plus (Invitrogen) as described (29). Transfection efficiency was determined by quantitative PCR (qPCR) and Western blot analysis. All these cell lines were used within 10 passages after reception in the current experiments, and have been routinely tested for mycoplasma contamination using the PCR Mycoplasma Detection Kit (ABM) and the last mycoplasma test was performed in August 2017. Mycoplasma-free cell lines were used in all of our experiments.

Patient samples

Blood was taken prior to operation from 19 breast cancer patients who did not have any complications, and underwent surgery at Niigata University Medical and Dental Hospital. Serum was separated by centrifugation, and preserved at −180°C. All the patients were Japanese, and obesity was defined as body mass index (BMI) 25 kg/m^2 among that population. Collection and use of all specimens in this study were approved by the

Institutional Review Board of Niigata University. Written informed consent was obtained from all participants and the studies were conducted in accordance with the Declaration of Helsinki.

Animal models

All animal studies were conducted in the Animal Research Core Facility at VCU School of Medicine in accordance with the institutional guidelines. Animals were bred and maintained in a pathogen-free environment and all procedures were approved by the VCU Institutional Animal Care and Use Committee (IACUC) that is accredited by Association for Assessment and Accreditation of Laboratory Animal Care.

Female C57Bl/6 mice and BALB/c mice were obtained from Jackson Labs. Mice were fed with either normal diet (ND) or high-fat diet (HFD; TD.88137, Harlan Labs) containing cholesterol (0.2%), total fat (21% by weight; 42% kcal from fat), saturated fatty acids (>60% of total fatty acids), sucrose (34% by weight), protein (17.3% by weight), and carbohydrate (48.5% by weight) for 12 weeks prior to implantation of cancer cells. E0771 breast cancer cells (5×10^4 cells in 10-μL Matrigel) were surgically implanted in the upper mammary fat pad under direct visualization as described previously (23). Tumor size was measured with calipers every 2 days and total tumor volume was estimated by the cylinder formula. Tumor-bearing mice were randomized 2 days after implantation prior to treatment with saline or FTY720. FTY720 (Cayman Chemicals) was administered by gavage at a dose of 1 mg/kg/day in PBS. Mice were sacrificed by exsanguination, blood was collected, tumors excised, weighed, fixed in formalin, and embedded in paraffin or frozen in liquid nitrogen. For survival studies, mice were euthanized according to a morbidity scale approved by IACUC.

For tumor-conditioned media (TCM) treatments, mice were injected intraperitoneally with TCM (300 μL) from E0771, HeLa, or 4T1-luc2 cells overexpressing *Sphk1* or from vector-transfected cells for 5 days prior to tail vein injections of E0771 cells or 4T1 cells (1×10^5/100 μL/mouse), respectively, as described previously (19, 20, 30). Metastatic lesions in the lung were determined histologically, by examining hematoxyin and eosin (H&E)–stained sections.

For the spontaneously developed breast cancer model, male MMTV-PyMT mice on a FVB/N background (Jackson Laboratories) were randomly bred with normal FVB/N females to obtain females heterozygous for the PyMT oncogene. Female heterozygous mice developed palpable mammary tumors as early as 5 weeks of age. Tumor sizes were measured every 3 days by caliper and total tumor volume was estimated by the cylinder formula (31). HFD or ND feeding and FTY720 administration was started at weaning.

Bioluminescent quantification of tumor burden

D-Luciferin (0.2-mL of 15 mg/mL stock, PerkinElmer) was injected intraperitoneally into mice previously implanted with 4T1-luc2 cells, and Living Image Software (Xenogen) was used to quantify the photons/second emitted by the cells as described previously (23).

Interstitial fluid collection

Interstitial fluid (IF) from breast and breast tumors was collected as described previously (32, 33). Briefly, tissue was excised and placed in preweighed tubes on ice. Tubes were reweighed to determine tissue weight and the tissue was sectioned several times with scissors. Samples were then transferred into inserts capped with nylon mesh, and placed into preweighed centrifuge tubes. The tubes were centrifuged at 100 × *g* for 10 minutes at 4°C and the IF accumulated in the bottom. The volume of IF was quantified by weight. PBS containing phosphatase inhibitors (100 μL) was added to the IF and the tubes were centrifuged at 1,000 × *g* for 10 minutes at 4°C to remove any contaminating cells.

Quantification of S1P and dihydro-S1P by mass spectrometry

Lipids were extracted from blood, tissues, and interstitial fluid, and S1P and dihydro-S1P quantified by liquid chromatography, electrospray ionization-tandem mass spectrometry (LC-ESI-MS/MS, 4000 QTRAP, AB Sciex) as described previously (23, 34, 35).

Histopathologic analysis

Tissue slices (5 μm) were stained with H&E for morphologic analysis. Paraffin-embedded slides were deparaffinated, and antigen unmasking was carried out by microwave heating in citrate buffer for 20 minutes. Slides were incubated with 3% H_2O_2 and then with goat or horse serum (DAKO) for 30 minutes at room temperature. After washing with PBS, slides were incubated at 4°C overnight with the following primary antibodies with indicated dilutions: IL6 (1:200, Abcam), SphK1 (1:100, Abcam), S1PR1 (1:100, Santa Cruz Biotechnology), Ki67 (1:25, Dako). Biotinylated secondary antibodies (1:200) were added and incubated at room temperature for 20 minutes. After 5 minutes with streptavidin–HRP, sections were stained with DAB substrate and counterstained with hematoxylin. Slides were examined with a Zeiss Axioimager A1 (Jena) and images captured with an AxioCam MRc camera.

Immunofluorescence analysis

Tumors were also frozen, and embedded in optimal cutting medium (OCT 4583; Sakura Finetek) for immunofluorescence analysis. Sections were fixed in 4% paraformaldehyde, blocked with horse serum containing 2.5% of fraction V for 1 hour, and then stained with primary antibodies at 4°C overnight: anti–IL6 (1:200, Abcam), or anti-F4/80 (1:200, AbD Serotec). After two washes with PBS, sections were stained with Alexa488- and Alexa594-conjugated secondary antibodies (1:500, Invitrogen) for 30 minutes. Nuclei were counterstained with Hoechst 33432 (Invitrogen) for 5 minutes. Slides were mounted and examined with a LSM710 laser-scanning confocal microscope (Zeiss).

Immunoblotting

Frozen tissue samples were homogenized and sonicated in 300 μL of buffer containing 50 mmol/L HEPES (pH 7.4), 150 mmol/L NaCl, 1 mmol/L EDTA, 1% Triton X-100, 2 mmol/L sodium orthovanadate, 4 mmol/L sodium pyrophosphate, 100 mmol/L NaF, 1:500 protease inhibitor mixture (Sigma). Equal amounts of proteins were separated by SDS-PAGE, transblotted to nitrocellulose, and immunopositive bands visualized by ECL (36).

Real-time PCR

Total RNA was isolated from tissues and cells using TRIzol (Life Technologies) and reverse transcribed with the High Capacity cDNA Reverse Transcription Kit. Premixed primer-probe sets and TaqMan Universal PCR Master Mix (Applied Biosystems) were employed to examine mRNA levels. cDNAs were diluted 10-fold (for the target genes) or 100-fold (for GAPDH) and amplified using the ABI7900HT cycler. *Gapdh* mRNA was used as an internal mRNA was used as an internal control to normalize mRNA expression.

Statistical analysis

Statistical analysis was performed using unpaired two-tailed Student *t* test for comparison of two groups and ANOVA followed by *post hoc* tests for multiple comparisons (GraphPad Prism). $P < 0.05$ was considered significant. Experiments were repeated at least three times in triplicate with consistent results. *In vivo* experiments were repeated three times and each experimental group consisted of at least six mice.

Results

Obesity increases S1P levels in breast cancer patients and in a syngeneic breast cancer model

Because obesity is now recognized as an independent prognostic factor for breast cancer patients (37, 38), and we have shown that S1P levels are elevated in breast tumors (23), it was of interest to examine the effects of obesity on S1P levels in breast cancer patients that did not yet receive therapy. S1P levels in serum from obese breast cancer patients were significantly higher than those from nonobese patients (Fig. 1A). Likewise, serum levels of dihydro-S1P, which also binds to all S1P receptors, were significantly higher in the obese patients (Fig. 1A).

Next, HFD induced obesity in C57Bl/6 mice, a common model because of its similarities to metabolic changes in obese humans, was used to investigate the mechanisms underlying obesity-promoted breast cancer progression. To this end, E0771 mouse breast cancer cells were implanted into mammary fat pad of syngeneic C57Bl/6 mice fed with HFD or ND for 12 weeks (Fig. 1B). As expected, mice fed with HFD developed significantly larger tumors within 30 days than those on ND (Fig. 1C). HFD significantly increased S1P levels in both normal mammary fat pad and breast tumors (Fig. D). HFD also significantly increased S1P levels in the tumor IF, which is a component of the tumor microenvironment and bathes cancer cells in the tumor (Fig. 1D). This is in agreement with our previous finding that tumor generated S1P is secreted into tumor IF (33), and that S1P levels are higher in human breast cancer and its tumor IF compared with those of normal breast tissue (33, 39). Similar to patients, levels of S1P in serum from nontumor-bearing mice and tumor-bearing mice fed with HFD were also significantly increased compared with mice on ND, and the difference between mice fed with ND and those with HFD were larger in the tumor bearing mice than nontumor-bearing mice (Fig. 1D). Moreover, S1P levels in the lung were also increased in the mice fed with HFD regardless of tumor existence (Fig. 1D). Consistent with elevation of S1P in tumors, expression of SphK1, but not SphK2, and S1PR1, albeit to a much lesser extent, was increased in the tumors from mice fed HFD (Fig. 1E).

The SphK1/S1P/S1PR1 axis connects obesity, chronic inflammation, and breast cancer progression

To investigate the involvement of the S1P/S1PR1 axis in tumor progression in obese animals, we utilized the prodrug FTY720/fingolimod that is phosphorylated *in vivo* to its active form FTY720-P, an S1P mimetic that acts as a functional antagonist of S1PR1 by inducing its internalization and degradation (40). When E0771 tumors in syngeneic mice on a HFD reached 5 mm in diameter, mice were treated orally daily with FTY720 (1 mg/kg) or saline. FTY720 significantly suppressed tumor progression determined by decreases of primary tumor volumes and tumor weights in the obese mice (Fig. 2A and B). FTY720 administration, however, did not significantly affect weight gain of HFD-fed mice (Fig. 2C), indicating that FTY720 did not affect diet intake. Treatment with FTY720 also significantly suppressed HFD-induced elevation of S1P in serum, tumors, and IF (Fig. 2D).

The proinflammatory cytokines, IL6 and TNFα, produced by tumor-infiltrating stromal cells, such as TAMs, are known to have important roles in obesity-related cancer progression (12). Indeed, expression of these cytokines was increased in the tumors of HFD-fed mice, compared with those fed ND, which was suppressed by FTY720 treatment (Fig. 2E). Moreover, as expected, HFD increased recruitment of TAMs, as revealed by immunofluorescence with anti-F4/80, (Fig. 2F). Of note, FTY720 dramatically decreased infiltration of TAMs in tumors of HFD-fed mice (Fig. 2F).

Targeting the SphK1/S1P/S1PR1 axis with FTY720 attenuates obesity-induced tumor progression and inflammation

An obesogenic HFD has been shown to enhance primary tumorigenesis and metastasis in MMTV-PyMT transgenic mice, which spontaneously develop breast cancer accompanied by recruitment of TAMs and increased tissue inflammation (9, 10). Therefore, we also sought to examine the role of the SphK1/S1P/S1PR1 axis in the link between inflammation and obesity-promoted breast cancer progression in this mouse model that closely mimics progression of the human disease (41). Consistent with previous reports (7–10, 31), HFD increased tumor incidence, multiplicity, and size with a significant increase in proliferation determined by Ki67 staining (Fig. 3A and B). HFD feeding, which increased circulating S1P levels (Fig. 3C), also enhanced mRNA expression of SphK1, but not SphK2, and S1PR1 in tumors, corresponding with increased protein levels determined by IHC (Fig. 3D and E). Because we and others have shown that enhanced S1PR1 expression reciprocally activates STAT3, leading to its persistent activation and upregulation of IL6 expression (36, 42), we also studied the effects of interfering with S1P formation and S1PR1 function and this feed-forward amplification loop with FTY720. Daily administration of FTY720 to HFD-fed MMTV-PyMT transgenic mice not only decreased HFD-induced S1PR1 expression, but also, in agreement with the notion that it is an inhibitor of SphK1 and induces its proteasomal degradation (43, 44), FTY720 almost completely abrogated the increase in SphK1 protein in the tumors (Fig. 3D and E). Concomitantly, FTY720 administration prevented increased levels of circulating S1P (Fig. 3C), prevented activation of Stat3, and increases in IL6 expression, and reduced tumor development of HFD-fed MMTV-PyMT mice (Fig. 3).

S1P produced by tumor SphK1 primes distant premetastatic sites

Our results show that S1P is secreted from the primary tumor into the tumor IF that drains into systemic circulation via lymphatic flow. Taken together with a recent study suggesting that S1P transported out of lymph endothelial cells by Spns2 can regulate metastatic colonization (45), it was intriguing to examine whether increased levels of circulating S1P can also promote formation of “premeta-static niches” in distant sites, such as the lung, that assist circulating cancer cells to form metastatic lesions at that location. To this end, prior to tail vein injections of E0771 breast cancer cells (Fig. 4A), mice were treated for 5 days with TCM from control or SphK1-overexpressing E0771 cells that contained increased levels of S1P (Fig. 4A; Supplementary Fig. S1).

Seven days after tumor challenge when there were no significant metastases, H&E staining showed extensive infiltration of inflammatory cells into the lungs of mice receiving TCM containing high levels of S1P (TCM-*Sphk1*) compared with those receiving control TCM (Fig. 4B). Histologic analysis also revealed extensive clusters of macrophages and greater IL6 staining (Fig. 4C). *Sphk1*, *S1pr1*, and *IL6* mRNA levels were also all significantly higher in those lungs (Fig. 4D). Furthermore, treating mice with TCM generated from SphK1-expressing tumor cells, but not TCM derived from control tumor cells, activated ERK, Akt, and STAT3 (Fig. 4E), known survival signaling pathways downstream of S1P/S1PR1, that have been implicated in premetastatic niche formation (19, 36, 42). We confirmed our findings by repeating experiments utilizing tail vein injections of another breast cancer cell line of 4T1-luc2 after 5-day TCM treatment. As expected, histologic analysis revealed that there were increased metastatic foci in the lung in the mice treated with TCM-*Sphk1* compared with those treated with control TCM (Fig. 4F).

FTY720 inhibits HFD-induced inflammation and lung-seeding ability for breast cancer cells

Because low-grade inflammation is induced by cancer, and obesity may exacerbate that inflammation, obesity has been suggested to increase cancer cell colonization and promote pulmonary breast cancer metastasis (6, 9, 10, 46). We next examined the involvement of the SphK1/S1P/S1PR1 axis in lung seeding ability for breast cancer cells. We performed tail vein injections of 4T1-luc2 cells after 5-day TCM-*Sphk1* treatment, and treated with clinically relevant doses of FTY720 (Fig. 5A), and found that FTY720 significantly decreased the tumor burden detected by IVIS imaging (Fig. 5B). To examine the effect of HFD, mice were fed HFD or ND for 12 weeks prior to treatment with TCM-*Sphk1* and subsequent intravenous injection of E0771 cells (Fig. 5C). The lungs of HFD-fed mice were heavier than those of mice fed ND, suggesting the presence of increased cancer cell–seeding lesions (Fig. 5D). Indeed, histologic analyses showed significantly increased numbers of cancer cell–seeding foci in the lungs of the HFD-fed mice (Fig. 5E). Moreover, HFD-induced obesity also increased recruitment of macrophages (Fig. 5F) that have been shown to mediate inflammatory responses, and increase expression of IL6 (Fig. 5F), which facilitate tumor cell recruitment, extravasation, and colonization into the niche (42, 46). S1P-stimulated signaling including pERK, pAKT, and pStat3, was also enhanced in lungs of mice fed HFD compared with ND (Fig. 5G). Importantly, treatment of mice fed HFD with clinically relevant doses of FTY720 dramatically suppressed HFD-induced formation of cancer cell–seeding foci (Fig. 5D and E), IL6, and macrophage infiltration (Fig. 5F), as well

as S1P-mediated signaling pathways (Fig. 5G). Finally, we repeated experiments utilizing tail vein injections of 4T1-luc2 cells after 5-day TCM-*Sphk1* treatment into HFD-fed mice, and treated with FTY720 (Fig. 5H). We found significant decreases of tumor burden in the mice treated with FTY720 compared with control mice (Fig. 5H).

FTY720 suppresses pulmonary metastasis in MMTV-PyMT transgenic and E0771 syngeneic orthotopic HFD-fed mice

In the metastatic lung colonization assay, cancer cells are injected intravenously and travel directly to the lung rather than from the primary tumor. Accordingly, we next tested the effect of FTY720 on obesity-related cancer metastasis of spontaneous and syngeneic breast tumors where cancer cells metastasize from the breast to the lung, more closely mimicking the pathology of the human disease. HFD enhanced pulmonary metastasis in MMTV-PyMT mice (Fig. 6A), consistent with previous reports (47). FTY720 administration drastically reduced lung metastases (Fig. 6A). Likewise, increased metastasis of breast cancer cells to the lung from E0771 orthotopic breast tumors was observed in mice fed HFD compared with those fed ND (Fig. 6B), with expression of SphK1 and S1PR1 significantly elevated in those lungs (Fig. 6C). Treatment of HFD-fed mice with FTY720 significantly reduced metastasis as well as expression of SphK1 and S1PR1 (Fig. 6B and C), indicating that elevated SphK1/S1P/S1PR1 correlates with HFD increased lung metastasis.

FTY720 suppresses obesity-related inflammation and S1P signaling and prolongs survival in tumor-bearing mice

The key inflammatory cytokine IL6, which is known to enhance metastatic potentials of tumor cells (46), was elevated in lungs from HFD-fed mice (Fig. 7A) concomitantly with increased S1P levels (Fig. 7B) and activation of key signaling pathways (Fig. 7C). FTY720 suppressed elevation of the proinflammatory cytokines, S1P levels, and stimulation of signaling pathways downstream of S1PR1 as demonstrated by reduction in phosphorylation of ERK, AKT, Stat3, and p65 (Fig. 7A–C). To determine whether FTY720 treatment also affects the survival of mice developing breast cancer lung metastases, we carried out a long-term study of syngeneic mice orthotopically implanted with E0771 cells. In agreement with previous studies in other animal models of breast cancer (48), Kaplan–Meier survival analysis revealed that HFD significantly worsened the survival of these mice compared with those fed ND (Fig. 7D). Daily administration of FTY720 significantly prolonged the survival of HFD-fed mice (Fig. 7D).

Discussion

Obesity-induced chronic inflammation has decisive roles in the pathogenesis of breast cancer and distal recurrence; however, the underlying mechanisms linking obesity and chronic inflammation to an increased risk of breast cancer and metastasis are poorly understood. In the current study, we identified a novel mechanism involving the SphK1/S1P/S1PR1 axis in a malevolent feed-forward amplification loop that connects obesity, inflammation, and breast cancer progression and metastasis. Targeting this axis with FTY720, which reduced expression of SphK1 and S1PR1 and S1P levels, significantly suppressed breast cancer metastasis and prolonged survival in obese HFD-fed MMTV-

PyMT transgenic and E0771 syngeneic orthotopic breast cancer mice. In agreement with the critical role of the SphK1/S1P/S1PR1 axis in persistent activation of NFκB and STAT3 and production of proinflammatory cytokines IL6 and TNFα (19, 36, 42), we found that in animals bearing breast tumors, increased S1P by HFD is essential for the production of IL6, the multifunctional NFκB-regulated cytokine, as well as activation of STAT3 and the upregulation of its target gene *S1pr1* (36). Administration of FTY720 interfered with the SphK1/S1P/S1PR1 axis and prevented STAT3 activation along with decreasing these proinflammatory cytokines and macrophage recruitment, resulting in suppression of obesity-promoted chronic inflammation and breast cancer progression and metastasis.

We have revealed that HFD increases S1P levels in the circulation of not only tumor-bearing animals, but also of nontumor-bearing animals (Fig. 1). Furthermore, S1P levels in the normal mammary fat pad and lung tissue were also increased with HFD without tumor. These findings indicate that obesity itself increase the levels of S1P in the body. Indeed, it has been reported that S1P levels are positively associated with obesity in humans. Plasma levels of S1P were reported to be higher in obese patients than those in nonobese and lean individuals (49). In addition, it was demonstrated that levels of plasma S1P directly correlate with BMI and total body fat percentage (28, 50). Taken together, these findings indicate that the S1P levels in the blood and local organs are increased with obesity most likely in addition to increased S1P secretion from enlarged tumor.

Our data show that HFD-induced obesity increased levels of S1P not only in the primary tumor itself but also in tumor interstitial fluid—a component of the tumor microenvironment, in the systemic circulation, and in distant sites such as the lungs. Similarly, serum S1P levels from obese breast cancer patients are higher than those in normal weight patients. The “seed-and-soil hypothesis,” first proposed by Paget, spawned the idea that primary tumors secrete factors that contribute to the development of premetastatic niches, characterized by an abundance of bone marrow–derived cells and stromal cells (30, 51). It has also been shown that even before tumor cells arrive premetastatic niches in distant organs are formed to create a favorable microenvironment for disseminating tumor cell colonization (52). Our data suggest that S1P is one of these factors secreted by tumor cells due to upregulation of SphK1. We found that TCM from SphK1-overexpressing breast cancer cells, which contains high levels of S1P, promoted metastatic niche formation and lung metastasis. S1PR1 has previously been identified as a key component for persistent activation of STAT3 in both primary tumors and in various cell types including myeloid cells in distant organs, leading to premetastatic niche formation (19, 42). Although in the past it was not clear how S1PR1 was activated, our results suggest that S1P secretion from tumor cells is the primary driver of S1PR1 activation to influence the microenvironment of distant organs such as lung by promoting recruitment of macrophages known to promote tumor cell extravasation, seeding, and persistent growth, and enabling metastasis (Fig. 7E). Consistent with this key role for S1P, a genome-wide screening of 800 mutant mice using an *in vivo* assay for the discovery of new microenvironmental regulators of metastatic colonization identified the S1P transporter Spns2 that regulates levels of S1P in lymph and blood as a critical new player (45).

We also found that in HFD-induced obese animals, SphK1 and S1PR1 expression is increased in metastatic lesions, along with higher levels of proinflammatory cytokines, IL6 and TNFα. Taken together with previous findings, this indicates that upregulation of SphK1, formation of S1P, and subsequent activation of S1PR1 leads to persistent activation of survival signaling and STAT3 in a malicious feed-forward amplification loop critical for breast cancer proliferation, survival, crosstalk with the microenvironment and metastasis.

FTY720, which targets the SphK1/S1P/S1PR1 axis, prevents the amplification cascade and mitigates obesity-promoted metastatic niche formation and breast cancer metastasis. We found that FTY720 decreased S1P levels as well as SphK1 and S1PR1 expression in the breast tumors. It has been reported that FTY720 inhibits SphK1 activity and promotes its proteosomal degradation (53). It has also been reported that FTY720 induces functional antagonism by the rapid polyubiquitylation, endocytosis, and proteasomal degradation of S1PR1 (54). This mechanism may also contribute to FTY720-induced cancer cell–selective apoptosis (55) and its inhibition of tumor vascularization and angiogenesis (56). Taken together, these direct effects of FTY720 on sphingolipid metabolism may explain the mechanisms through which FTY720 targets the SphK1/S1P/S1PR1 axis.

It is possible that the reduction of primary tumor size may be at least partly responsible for the decrease of metastatic tumor burden. Although our results of survival data (Fig. 7) showed a benefit from FTY720, the effect was not as dramatic as the results shown in Figs. 4–6. In this case, response to therapy was not linear to the length of survival. While the reduction in disease burden substantiates an important role for the SphK1/S1P/S1PR1 axis, there remained a significant disease burden in treated mice, implying limited efficacy as a single modality therapy. Clinically, it is well known that therapies that reduce metastatic burden often do not result in longer survival in a variety of settings of human patients (57).

Our objective is to elucidate the role of the SphK1/S1P/S1PR1 axis in cancer associated with inflammation and to show the effects of FTY720 in that setting. FTY720 acts by multiple means in addition to its effects on obesity-related inflammation. In agreement with previous reports, we also found that FTY720 inhibited tumor growth in mice treated with ND. In this research, our discovery is that FTY720 is effective on cancer with obesity-associated inflammation. Future development of more specific drugs that target the SphK1/S1P/S1PR1 axis will further aid in elucidating its importance in control of pulmonary metastatic burden and the usefulness of targeting this axis therapeutically for obesity-promoted metastatic breast cancer.

Supplementary Material

Refer to Web version on PubMed Central for supplementary material.

Acknowledgments

The VCU Lipidomics and Microscopy Cores are supported in part by funding from the NIH-NCI Cancer Center Support Grant P30 CA016059. M. Nagahashi was a Japan Society for the Promotion of Science Postdoctoral Fellow. M. Nagahashi is supported by the Japan Society for the Promotion of Science (JSPS) Grant-in-Aid for Scientific Research Grant Number 15H05676 and 15K15471, the Uehara Memorial Foundation, Nakayama Cancer Research Institute, Takeda Science Foundation, and Tsukada Medical Foundation. T. Wakai is supported by the

JSPS Grant-in-Aid for Scientific Research Grant Number 15H04927 and 16K15610. K. Takabe is supported by NIH/NCI grant R01CA160688 and Susan G. Komen Investigator Initiated Research Grant IIR12222224. S. Spiegel is supported by the Department of Defense BCRP Program Award (W81XWH-14-1-0086). K.P. Terracina was supported by T32CA085159.

References

1. Flegal KM, Carroll MD, Ogden CL, Curtin LR. Prevalence and trends in obesity among US adults, 1999–2008. JAMA 2010;303: 235–41. [PubMed: 20071471]
2. Calle EE, Rodriguez C, Walker-Thurmond K, Thun MJ. Overweight, obesity, and mortality from cancer in a prospectively studied cohort of U.S. adults. N Engl J Med 2003;348:1625–38. [PubMed: 12711737]
3. Niraula S, Ocana A, Ennis M, Goodwin PJ. Body size and breast cancer prognosis in relation to hormone receptor and menopausal status: a meta-analysis. Breast Cancer Res Treat 2012;134:769–81. [PubMed: 22562122]
4. Neuhouser ML, Aragaki AK, Prentice RL, Manson JE, Chlebowski R, Carty CL, et al. Overweight, obesity, and postmenopausal invasive breast cancer risk: a secondary analysis of the women's health initiative randomized clinical trials. JAMA Oncol 2015;1:611–21. [PubMed: 26182172]
5. Demark-Wahnefried W, Platz EA, Ligibel JA, Blair CK, Courneya KS, Meyerhardt JA, et al. The role of obesity in cancer survival and recurrence. Cancer Epidemiol Biomarkers Prev 2012;21:1244–59. [PubMed: 22695735]
6. Fuentes-Mattei E, Velazquez-Torres G, Phan L, Zhang F, Chou PC, Shin JH, et al. Effects of obesity on transcriptomic changes and cancer hallmarks in estrogen receptor-positive breast cancer. J Natl Cancer Inst 2014;106. doi: 10.1093/jnci/dju158.
7. La Merrill M, Gordon RR, Hunter KW, Threadgill DW, Pomp D. Dietary fat alters pulmonary metastasis of mammary cancers through cancer autonomous and non-autonomous changes in gene expression. Clin Exp Metast 2010;27:107–16.
8. Llaverias G, Danilo C, Mercier I, Daumer K, Capozza F, Williams TM, et al. Role of cholesterol in the development and progression of breast cancer. Am J Pathol 2011;178:402–12. [PubMed: 21224077]
9. Sundaram S, Yan L. High-fat diet enhances mammary tumorigenesis and pulmonary metastasis and alters inflammatory and angiogenic profiles in MMTV-PyMT mice. Anticancer Res 2016;36: 6279–87. [PubMed: 27919947]
10. Cowen S, McLaughlin SL, Hobbs G, Coad J, Martin KH, Olfert IM, et al. High-fat, high-calorie diet enhances mammary carcinogenesis and local inflammation in MMTV-PyMT mouse model of breast cancer. Cancers 2015;7:1125–42. [PubMed: 26132316]
11. Maccio A, Madeddu C. Obesity, inflammation, and postmenopausal breast cancer: therapeutic implications. Scientific World Journal 2011; 11:2020–36. [PubMed: 22125453]
12. Khandekar MJ, Cohen P, Spiegelman BM. Molecular mechanisms of cancer development in obesity. Nat Rev Cancer 2011;11:886–95. [PubMed: 22113164]
13. Antonioli L, Blandizzi C, Pacher P, Hasko G. Immunity, inflammation and cancer: a leading role for adenosine. Nat Rev Cancer 2013; 13:842–57. [PubMed: 24226193]
14. Chang CC, Wu MJ, Yang JY, Camarillo IG, Chang CJ. Leptin-STAT3-G9a signaling promotes obesity-mediated breast cancer progression. Cancer Res 2015;75:2375–86. [PubMed: 25840984]
15. Donohoe CL, Lysaght J, O'Sullivan J, Reynolds JV. Emerging concepts linking obesity with the hallmarks of cancer. Trends Endocrinol Metab 2017;28:46–62. [PubMed: 27633129]
16. Feola A, Ricci S, Kouidhi S, Rizzo A, Penon A, Formisano P, et al. Multi-faceted breast cancer: the molecular connection with obesity. J Cell Physiol 2017;232:69–77. [PubMed: 27363538]
17. Sundaram S, Johnson AR, Makowski L. Obesity, metabolism and the microenvironment: Links to cancer. J Carcinogenesis 2013;12:19.
18. Psaila B, Lyden D. The metastatic niche: adapting the foreign soil. Nat Rev Cancer 2009;9:285–93. [PubMed: 19308068]

19. Deng J, Liu Y, Lee H, Herrmann A, Zhang W, Zhang C, et al. S1PR1-STAT3 signaling is crucial for myeloid cell colonization at future metastatic sites. Cancer Cell 2012;21:642–54. [PubMed: 22624714]
20. Sceneay J, Chow MT, Chen A, Halse HM, Wong CS, Andrews DM, et al. Primary tumor hypoxia recruits CD11b+/Ly6Cmed/Ly6G+ immune sup pressor cells and compromises NK cell cytotoxicity in the premetastatic niche. Cancer Res 2012;72:3906–11. [PubMed: 22751463]
21. Aoyagi T, Nagahashi M, Yamada A, Takabe K. The role of sphingosine-1-phosphate in breast cancer tumor-induced lymphangiogenesis. Lymphat Res Biol 2012;10:97–106. [PubMed: 22984905]
22. Pyne NJ, Pyne S. Sphingosine 1-phosphate and cancer. Nat Rev Cancer 2010;10:489–503. [PubMed: 20555359]
23. Nagahashi M, Ramachandran S, Kim EY, Allegood JC, Rashid OM, Yamada A, et al. Sphingosine-1-phosphate produced by sphingosine kinase 1 promotes breast cancer progression by stimulating angiogenesis and lymphangiogenesis. Cancer Res 2012;72:726–35. [PubMed: 22298596]
24. Takabe K, Spiegel S. Export of sphingosine-1-phosphate and cancer progression. J Lipid Res 2014;55:1839–46. [PubMed: 24474820]
25. Nagahashi M, Yuza K, Hirose Y, Nakajima M, Ramanathan R, Hait NC, et al. The roles of bile acids and sphingosine-1-phosphate signaling in the hepatobiliary diseases. J Lipid Res 2016;57:1636–43. [PubMed: 27459945]
26. Ruckhaberle E, Rody A, Engels K, Gaetje R, von Minckwitz G, Schiffmann S, et al. Microarray analysis of altered sphingolipid metabolism reveals prognostic significance of sphingosine kinase 1 in breast cancer. Breast Cancer Res Treat 2008;112:41–52. [PubMed: 18058224]
27. Tsuchida J, Nagahashi M, Nakajima M, Moro K, Tatsuda K, Ramanathan R, et al. Breast cancer sphingosine-1-phosphate is associated with phospho-sphingosine kinase 1 and lymphatic metastasis. J Surg Res 2016;205:85–94. [PubMed: 27621003]
28. Kowalski GM, Carey AL, Selathurai A, Kingwell BA, Bruce CR. Plasma sphingosine-1-phosphate is elevated in obesity. PLoS One 2013;8: e72449. [PubMed: 24039766]
29. Paugh SW, Paugh BS, Rahmani M, Kapitonov D, Almenara JA, Kordula T, et al. A selective sphingosine kinase 1 inhibitor integrates multiple molecular therapeutic targets in human leukemia. Blood 2008;112: 1382–91. [PubMed: 18511810]
30. Kaplan RN, Riba RD, Zacharoulis S, Bramley AH, Vincent L, Costa C, et al. VEGFR1-positive haematopoietic bone marrow progenitors initiate the pre-metastatic niche. Nature 2005;438:820–7. [PubMed: 16341007]
31. Hait NC, Avni D, Yamada A, Nagahashi M, Aoyagi T, Aoki H, et al. The phosphorylated prodrug FTY720 is a histone deacetylase inhibitor that reactivates ERalpha expression and enhances hormonal therapy for breast cancer. Oncogenesis 2015;4:e156. [PubMed: 26053034]
32. Nagahashi M, Kim EY, Yamada A, Ramachandran S, Allegood JC, Hait NC, et al. Spns2, a transporter of phosphorylated sphingoid bases, regulates their blood and lymph levels, and the lymphatic network. FASEB J 2013;27:1001–11. [PubMed: 23180825]
33. Nagahashi M, Yamada A, Miyazaki H, Allegood JC, Tsuchida J, Aoyagi T, et al. Interstitial fluid sphingosine-1-phosphate in murine mammary gland and cancer and human breast tissue and cancer determined by novel methods. J Mammary Gland Biol Neoplasia 2016;21:9–17. [PubMed: 27194029]
34. Hait NC, Allegood J, Maceyka M, Strub GM, Harikumar KB, Singh SK, et al. Regulation of histone acetylation in the nucleus by sphingosine-1-phosphate. Science 2009;325:1254–7. [PubMed: 19729656]
35. Takabe K, Kim RH, Allegood JC, Mitra P, Ramachandran S, Nagahashi M, et al. Estradiol induces export of sphingosine 1-phosphate from breast cancer cells via ABCC1 and ABCG2. J Biol Chem 2010;285:10477–86. [PubMed: 20110355]
36. Liang J, Nagahashi M, Kim EY, Harikumar KB, Yamada A, Huang WC, et al. Sphingosine-1-phosphate links persistent STAT3 activation, chronic intestinal inflammation, and development of colitis-associated cancer. Cancer Cell 2013;23:107–20. [PubMed: 23273921]

37. Ewertz M, Gray KP, Regan MM, Ejlertsen B, Price KN, Thurlimann B, et al. Obesity and risk of recurrence or death after adjuvant endocrine therapy with letrozole or tamoxifen in the breast international group 1–98 trial. J Clin Oncol 2012;30:3967–75. [PubMed: 23045588]
38. Sinicrope FA, Dannenberg AJ. Obesity and breast cancer prognosis: weight of the evidence. J Clin Oncol 2011;29:4–7. [PubMed: 21115867]
39. Nagahashi M, Tsuchida J, Moro K, Hasegawa M, Tatsuda K, Woelfel IA, et al. High levels of sphingolipids in human breast cancer. J Surg Res 2016; 204:435–44. [PubMed: 27565080]
40. Brinkmann V, Billich A, Baumruker T, Heining P, Schmouder R, Francis G, et al. Fingolimod (FTY720): discovery and development of an oral drug to treat multiple sclerosis. Nat Rev Drug Discov 2010;9:883–97. [PubMed: 21031003]
41. Maglione JE, Moghanaki D, Young LJ, Manner CK, Ellies LG, Joseph SO, et al. Transgenic Polyoma middle-T mice model premalignant mammary disease. Cancer Res 2001;61:8298–305. [PubMed: 11719463]
42. Lee H, Deng J, Kujawski M, Yang C, Liu Y, Herrmann A, et al. STAT3-induced S1PR1 expression is crucial for persistent STAT3 activation in tumors. Nat Med 2010;16:1421–8. [PubMed: 21102457]
43. Lim KG, Tonelli F, Li Z, Lu X, Bittman R, Pyne S, et al. FTY720 analogues as sphingosine kinase 1 inhibitors: enzyme inhibition kinetics, allosterism, proteasomal degradation, and actin rearrangement in MCF-7 breast cancer cells. J Biol Chem 2011;286:18633–40. [PubMed: 21464128]
44. Tonelli F, Lim KG, Loveridge C, Long J, Pitson SM, Tigyi G, et al. FTY720 and (S)-FTY720 vinylphosphonate inhibit sphingosine kinase 1 and promote its proteasomal degradation in human pulmonary artery smooth muscle, breast cancer and androgen-independent prostate cancer cells. Cell Signal 2010;22:1536–42. [PubMed: 20570726]
45. van der Weyden L, Arends MJ, Campbell AD, Bald T, Wardle-Jones H, Griggs N, et al. Genome-wide in vivo screen identifies novel host regulators of metastatic colonization. Nature 2017;541:233–6. [PubMed: 28052056]
46. Liu Y, Cao X. Characteristics and significance of the pre-metastatic Niche. Cancer Cell 2016;30:668–81. [PubMed: 27846389]
47. Gluschnaider U, Hertz R, Ohayon S, Smeir E, Smets M, Pikarsky E, et al. Long-chain fatty acid analogues suppress breast tumorigenesis and progression. Cancer Res 2014;74:6991–7002. [PubMed: 25304261]
48. Kim EJ, Choi MR, Park H, Kim M, Hong JE, Lee JY, et al. Dietary fat increases solid tumor growth and metastasis of 4T1 murine mammary carcinoma cells and mortality in obesity-resistant BALB/c mice. Breast Cancer Res 2011;13:R78. [PubMed: 21834963]
49. Ito S, Iwaki S, Koike K, Yuda Y, Nagasaki A, Ohkawa R, et al. Increased plasma sphingosine-1-phosphate in obese individuals and its capacity to increase the expression of plasminogen activator inhibitor-1 in adipocytes. Coron Artery Dis 2013;24:642–50. [PubMed: 24212262]
50. Katsuta E, Yan L, Nagahashi M, Raza A, Sturgill JL, Lyon DE, et al. Doxorubicin effect is enhanced by sphingosine-1-phosphate signaling antagonist in breast cancer. J Surg Res 2017;219:202–13. [PubMed: 29078883]
51. Quail DF, Joyce JA. Microenvironmental regulation of tumor progression and metastasis. Nat Med 2013;19:1423–37. [PubMed: 24202395]
52. Kaplan RN, Rafii S, Lyden D. Preparing the “soil”: the premetastatic niche. Cancer Res 2006;66:11089–93. [PubMed: 17145848]
53. Valentine WJ, Kiss GN, Liu J, E S, Gotoh M, Murakami-Murofushi K, et al. (S)-FTY720-vinylphosphonate, an analogue of the immunosuppressive agent FTY720, is a pan-antagonist of sphingosine 1-phosphate GPCR signaling and inhibits autotaxin activity. Cell Signal 2010;22: 1543–53. [PubMed: 20566326]
54. Graler MH, Goetzl EJ. The immunosuppressant FTY720 down-regulates sphingosine 1-phosphate G-protein-coupled receptors. FASEB J 2004;18: 551–3. [PubMed: 14715694]
55. Azuma H, Horie S, Muto S, Otsuki Y, Matsumoto K, Morimoto J, et al. Selective cancer cell apoptosis induced by FTY720; evidence for a Bcl-dependent pathway and impairment in ERK activity. Anticancer Res 2003;23:3183–93. [PubMed: 12926052]

56. LaMontagne K, Littlewood-Evans A, Schnell C, O'Reilly T, Wyder L, Sanchez T, et al. Antagonism of sphingosine-1-phosphate receptors by FTY720 inhibits angiogenesis and tumor vascularization. Cancer Res 2006;66:221–31. [PubMed: 16397235]

57. Valachis A, Polyzos NP, Patsopoulos NA, Georgoulias V, Mavroudis D, Mauri D. Bevacizumab in metastatic breast cancer: a meta-analysis of randomized controlled trials. Breast Cancer Res Treat 2010;122:1–7. [PubMed: 20063120]

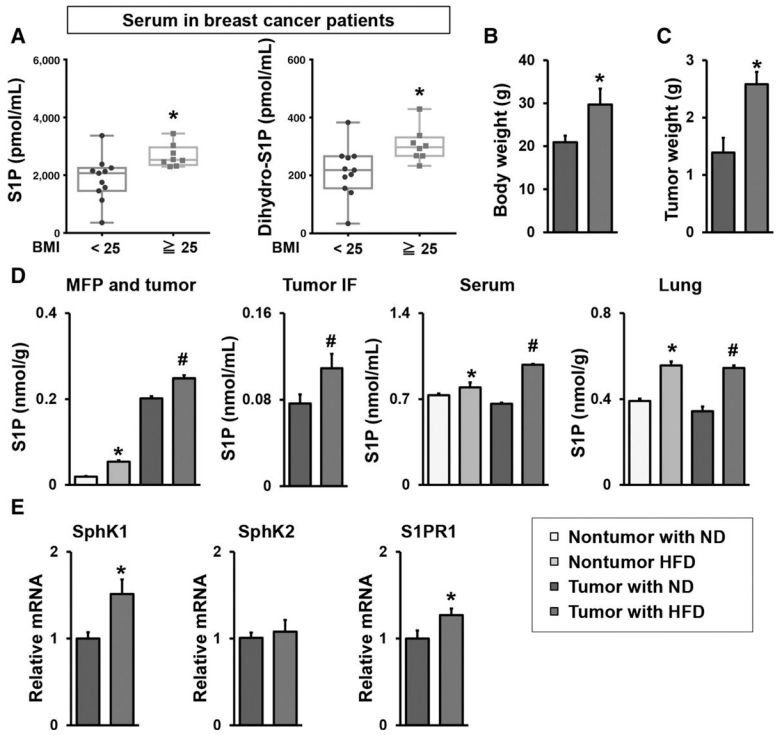

Figure 1.

Obesity increased circulating levels of S1P in humans and mice with breast cancer. **A,** S1P and dihydro-S1P levels in serum from preoperative breast cancer patients with BMI < 25 kg/m^2 (n = 11), or BMI 25 kg/m^2 (n = 8) were measured by LC-ESI-MS/MS. The S1P and dihydro-S1P levels are shown in the box plot. The central rectangle spans the first quartile to the third quartile. A segment inside the rectangle shows the median and "whiskers" above and below the box shows the value of the minimum and maximum. All data points are also shown as dots. *, P < 0.05. **B–E,** The SphK1/S1P/S1PR1 axis in HFD promoted breast cancer progression. **B,** Prior to implantation of E0771 cells into the chest mammary fat pad under direct vision, C57Bl/6 mice were fed ND or HFD for 12 weeks and body weight was measured. **C,** Tumors were harvested 30 days after the implantation, and the tumor weight was measured. Data are means ± SEM. *, P < 0.05. **D,**, Levels of S1P in mammary fat pad (MFP) and breast tumors, tumor IF, serum without or with breast tumors, and lung without or with breast tumors from mice fed with ND or HFD were measured by LC-ESI-MS/MS. **E,**, Expression of *Sphk1*, *Sphk2*, and *S1pr1* in breast tumors was determined by qPCR and normalized to *Gapdh* mRNA. Data are expressed as means ± SEM. *, P < 0.05.

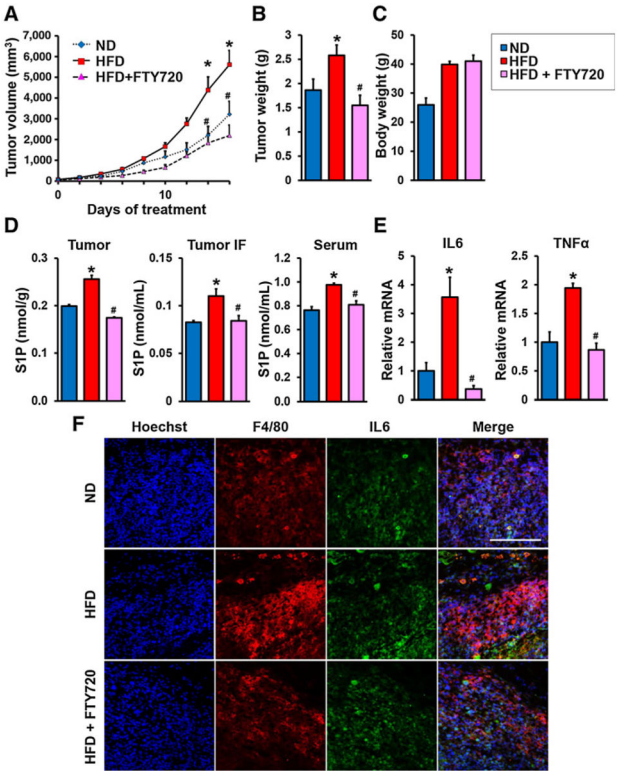

Figure 2.

The SphK1/S1P/S1PR1 axis connects obesity, chronic inflammation, and breast cancer progression. **A–E,** Mice were treated as above and when tumors reached 5 mm in diameter, HFD-fed mice were treated by gavage daily with PBS or FTY720 (1 mg/kg). **A,** Tumor volumes were measured on the indicated days. **B–E,** After treatment for 18 days, tumors were harvested and tumor and body weights determined (**B** and **C**). **D,** Levels of S1P in breast tumors, tumor IF, and serum were measured by LC-ESI-MS/MS. **E,** *Tnfα* and *IL6* mRNA levels in tumors were determined by qPCR and normalized to *Gapdh* mRNA. Data are expressed as means ± SEM. *, $P < 0.05$ versus ND; #, $P < 0.05$ versus HFD. **F,** Immunofluorescence analysis of tumors stained for IL6 (green), F4/80 (red), and Hoechst (blue). Scale bar, 100 μm.

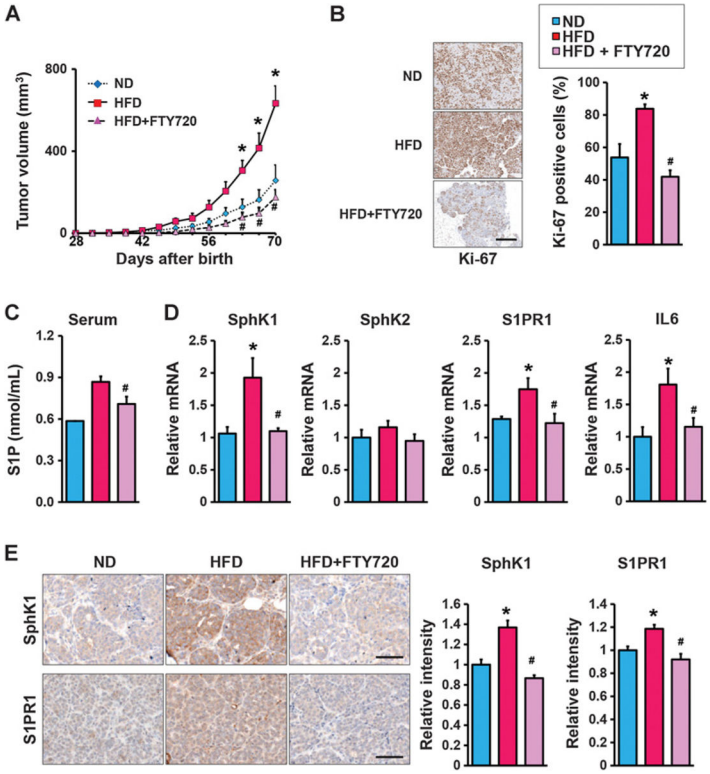

Figure 3.

Targeting the SphK1/S1P/S1PR1 axis with FTY720 mitigates HFD-induced inflammation and tumorigenesis in MMTV-PyMT transgenic mice. **A,** Beginning at 3 weeks of age, MMTV-PyMT transgenic mice were fed ND or HFD and treated daily by gavage with PBS or FTY720 (1 mg/kg). **A,** Spontaneous tumor sizes were determined on the indicated days. **B,** Tumor sections were stained with Ki67 antibody and percent Ki67–positive cells determined. Scale bar, 50 μm. **C,** Levels of S1P in serum were measured by LC-ESI-MS/MS. **D,** Expression of *Sphk1, Sphk2, S1pr1*, and *IL6* in breast tumors was determined by qPCR and normalized to *Gapdh* mRNA. **E,** Breast tumors were immunostained with anti-SphK1 or anti-S1PR1. Scale bar, 50 μm. Relative intensity of the immunostaining was quantified. Data are expressed as means ± SEM. *, $P < 0.05$ versus ND; #, $P < 0.05$ versus HFD.

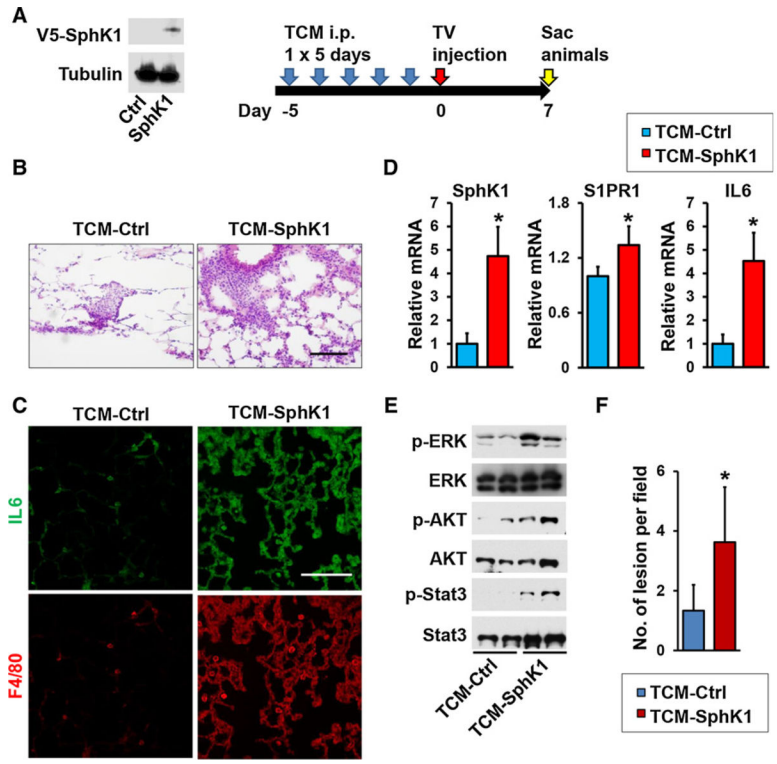

Figure 4.

S1P in tumor conditioned medium increased macrophage recruitment and induced factors and signaling pathways important for lung premetastatic niches. **A,** Equal amounts lysates of E0771 cells with SphK1 overexpression or control (Ctrl) analyzed by immunoblotting with the indicated antibodies (left). Schematic overview of regimen for examination of premetastatic niche formation in the lung utilizing TCM (right). **B–E,** Mice were treated with TCM from *Sphk1*-overexpressing E0771 cells (TCM-*Sphk1*) or control E0771 cells (TCM-Ctrl) for 5 days, followed by systemic tumor challenge. Lungs were harvested 7 days later. **B,** H&E staining of lung sections. Scale bar, 100 μm. **C,** Immunofluorescence analysis of lung sections stained for IL6 (green), F4/80 (red), and Hoechst (blue). Scale bar, 100 μm. **D,** Expression of *Sphk1*, *S1pr1*, and *IL6* mRNA in lungs determined by qPCR and normalized to levels of *Gapdh* mRNA. Data are means ± SEM. *, $P < 0.05$. **E,** Equal amounts of lung lysates analyzed by immunoblotting with the indicated antibodies. **F,** Quantitation of metastatic lesions in the mouse model with TV injection of 4T1-luc2. Data are means ± SD. *, $P < 0.05$ versus TCM-Ctrl.

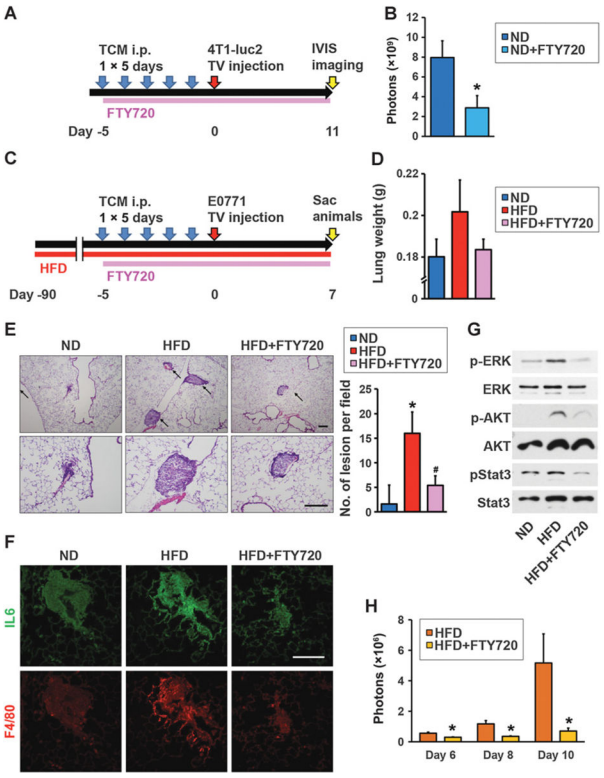

Figure 5.

FTY720 suppressed HFD-induced inflammation and lung-seeding ability of breast cancer cells. **A,** Schematic overview of treatment regimen for lung colonization. Mice were fed ND and treated with TCM from *Sphk1*-overexpressing 4T1-luc2 cells (TCM-*Sphk1*) for 5 days and also daily treated orally with PBS or with FTY720 (1 mg/kg) as indicated. At day 6, 4T1 cells were injected intravenously and tumor burden was quantified by *in vivo* bioluminescence on the indicated days. **B,** Tumor burden of mice with tail vein injection of 4T1-luc2 cells treated without or with FTY720 quantified by *in vivo* bioluminescence on day 11. Data are means ± SEM. *, $P < 0.05$ versus ND. **C,** Schematic overview of treatment regimen for lung colonization. Mice were fed ND or HFD for 12 weeks and treated with TCM from *Sphk1*-overexpressing E0771 cells (TCM-*Sphk1*) for 5 days and also daily treated orally with PBS or with FTY720 (1 mg/kg) as indicated. At day 6, E0771 cells were injected intravenously and 7 days later, lungs were harvested. **D,** Lung weights. **E,** H&E staining of lung sections. Top and bottom panels show lower (×40) and higher (×100) magnifications, respectively. Arrows, cancer cell–seeding lesions. Scale bar, 200 μm. Quantitation of cancer cell–seeding lesions. Data are means ± SEM. *, $P < 0.05$ versus ND; #, $P < 0.05$ versus HFD. **F,** Immunofluorescence analysis of lung sections stained for IL6 (green) and F4/80 (red). Scale bar, 100 μm. **G,** Equal amounts of lung lysates analyzed by immunoblotting, with the indicated antibodies. **H,** Tumor burden of HFD-fed mice with tail vein injection of 4T1-luc2 cells treated without or with FTY720 quantified by *in vivo* bioluminescence on the indicated days. Data are means ± SEM. *, $P < 0.05$ versus HFD, respectively.

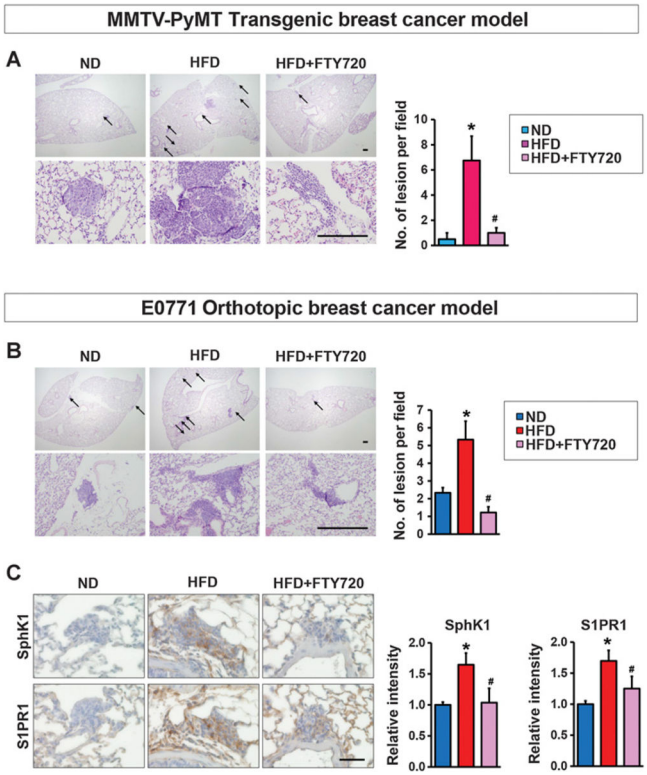

Figure 6.

FTY720 suppresses lung metastasis in HFD-fed MMTV-PyMT transgenic and E0771 syngeneic orthotopic breast cancer mice. **A,** MMTV-PyMT transgenic mice were fed with ND or HFD and treated daily by gavage with PBS or FTY720 (1 mg/kg) as indicated. Lungs were harvested when mice were 10 weeks old. **C,** H&E staining of lung sections. Top and bottom panels show lower (×20) and higher (×200) magnifications, respectively. Arrows, metastatic lesions. Scale bar, 100 μm. Quantitation of metastatic lesions. Data are means ± SEM. *, $P < 0.05$ versus ND; #, $P < 0.05$ versus HFD. **B** and **C,** C57Bl/6 mice were fed with ND or HFD for 12 weeks, before E0771 cells were implanted into the chest mammary fat pad under direct vision. When tumor sizes reached 5 mm in diameter, mice fed HFD were randomized into two groups and treated by gavage with PBS or FTY720 (1 mg/kg/day). Lungs were examined 18 days later. **B,** H&E staining of lung sections. Top and bottom panels show lower (×20) and higher (×200) magnifications, respectively. Arrows, metastatic lesions. Scale bar, 100 μm. Quantitation of metastatic lesions. Data are means ± SEM. *, $P < 0.05$ versus ND; #, $P < 0.05$ versus HFD. **C,** Lung sections were immunostained with anti-SphK1 or anti-S1PR1. Scale bar, 50 μm. Relative intensity of immunostaining was quantified. Data are means ± SEM. *, $P < 0.05$ versus PBS; #, $P < 0.05$ versus HFD.

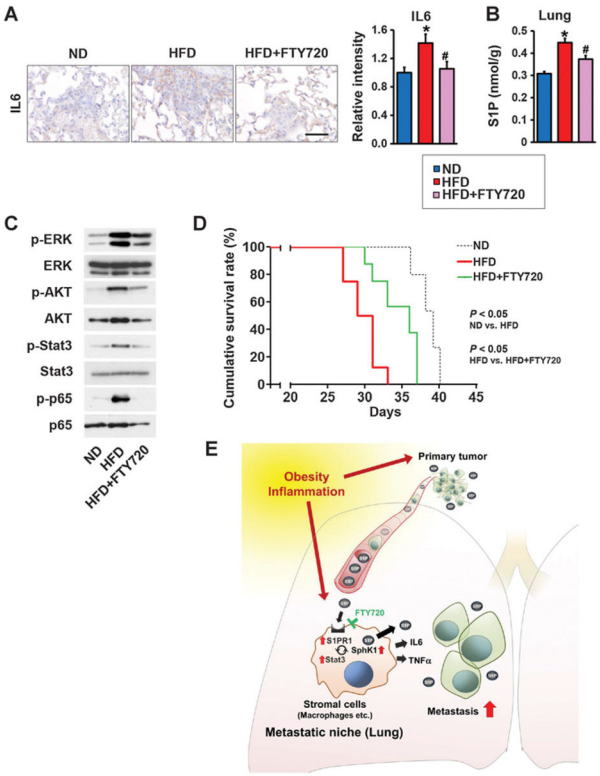

Figure 7.

FTY720 mitigates obesity-related lung inflammation and S1P signaling, and prolongs survival of breast cancer-bearing mice. **A–D,** C57Bl/6 mice were fed ND or HFD for 12 weeks. Tumor-bearing mice fed HFD were randomized into two groups 2 days after implantation and then treated by gavage with PBS or FTY720 (1 mg/kg/day) and 18 days later, lungs were examined. **A,** Lung sections were immunostained with anti-IL6. Scale bar, 50 μm. Relative intensity of the immunostaining was quantified. **B,** Levels of S1P in lungs were measured by LC-ESI-MS/MS. Data are means ± SEM. *, $P < 0.05$ versus. ND; #, $P < 0.05$ versus HFD. **C,** Equal amounts of lung lysates were analyzed by Western blotting with the indicated antibodies. **D,** Kaplan–Meier cumulative survival curves for mice fed with ND, HFD, or HFD plus FTY720 treatment. Data from days after E0771 implantation are shown. **E,** Scheme illustrating the role of SphK1/S1P/S1PR1 axis in the link between obesity, inflammation, and breast cancer progression and lung metastasis and targeting this axis with FTY720 for treatment. See text for more details.